Boundary Element Method for Solving the Two-dimensional Time-dependent Inverse Heat Conduction Problem

Somchart Chantasiriwan
Department of Mechanical Engineering, Faculty of Engineering
Thammasat University, Pathum Thani 12121, Thailand

Abstract

The unknown time-dependent boundary heat flux of a two-dimensional body is determined from temperature measurements inside the body or on its boundary. The method of solution is the boundary element method, which is used to obtain coefficients that relate unknown heat flux and measured temperatures. The quality of the estimated heat flux depends on how close it is to the actual heat flux and how sensitive it is to statistical errors in temperature measurements. The proposed method is used to solve a sample problem. It is shown that the number of heat flux components to be estimated, the number of temperature sensors, and the locations of the sensors influence the quality of the solution.

1. Introduction

The determination of unknown boundary heat flux of a solid body of which thermophysical properties are known from temperature measurements inside the body or on its boundary constitutes an inverse heat conduction problem (IHCP). A number of solution techniques have been proposed for the one-dimensional IHCP [1-4]. The two-dimensional IHCP, however, has received less attention so far [5-7] despite the fact that it can more realistically model practical problems than the one-dimensional IHCP.

The solution to IHCP often requires the determination of sensitivity coefficients [1]. For the one-dimensional IHCP, the sensitivity coefficients can be found in a straightforward manner due to the availability of the analytical solution to the corresponding direct problem. However, the analytical solution to the direct problem of two dimensions may be very complicated, and a numerical method such as the finite difference method or the finite element method must be employed in most cases. Since the finite element method can handle problems of arbitrary geometry efficiently, it has been proposed as the method for solving the two-dimensional IHCP [8].

Apart from the finite element method, another numerical method that is able to handle a general problem of arbitrary geometry is the boundary element method. For problems having no source term, the boundary element enjoys an important advantage over the finite element method in that no domain mesh generation is required. The boundary element method was previously used to solve the steady-state inverse heat conduction problem [9] and one-dimensional time-dependent IHCP [2]. In this paper, the two-dimensional time-dependent IHCP will be considered. The following sections will present the statement of the problem, the formulation of the boundary element method for solving the problem, and the solution of a sample problem by the proposed method. Discussion and conclusion will then follow.

2. Statement of the Problem

Consider a solid object with part of its boundary Γ_1 subjected to known heat flux and the remaining part of the boundary Γ_2 subjected to unknown heat flux. Suppose that the object has constant thermophysical properties, making the problem a linear one. Without the loss of generality, we can take the value of the thermal diffusivity to be unity and the initial condition to be uniformly zero. The heat conduction process can then be described by the following equations.

$$\frac{\partial T(\vec{r},t)}{\partial t} = \nabla^2 T(\vec{r},t) \qquad (1)$$

$$T(\vec{r},0) = 0 \quad (2)$$

$$\vec{n}\vec{\nabla}T(\vec{r},t)\Big|_{\Gamma_1} = g(\vec{r},t)\Big|_{\Gamma_1} \quad (3)$$

where $\vec{n}$ is the outward pointing unit vector normal to boundary and g is the known boundary heat flux. In order to render the problem solvable, the temperature measurement data must be specified.

$$T(\vec{r}_i, j\Delta t) = Y_i^{(j)} \quad (4)$$

where $\vec{r}_i$ is the position vector of a temperature sensor, and Δt is the measurement time step. Suppose that there are M_1 temperature sensors on the boundary and M_2 sensors inside the object. Furthermore, let Y_1, Y_2 ..., Y_{M_1} denote measurements on the boundary, and Y_{M_1+1}, Y_{M_1+2}, ..., $Y_{M_1+M_2}$ denote measurements inside the object.

3. Boundary Element Method

The formulation of the boundary element method for a time-dependent linear heat conduction problem is given by [10]

$$aT(\vec{\xi},t) = \int_\Gamma \int_0^t q(\vec{r},\tau)G(\vec{r}-\vec{\xi};t-\tau)\mathrm{d}\tau\mathrm{d}\vec{r} - \int_\Gamma \int_0^t T(\vec{r},\tau)\vec{n}\vec{\nabla}G(\vec{r}-\vec{\xi};t-\tau)\mathrm{d}\tau\mathrm{d}\vec{r} \quad (5)$$

where a depends on the location of $\vec{\xi}$, and the fundamental solution G is

$$G(\vec{r}-\vec{\xi};t-\tau) = \frac{\mathrm{e}^{-(\vec{r}-\vec{\xi})^2/4(t-\tau)}}{[4\pi(t-\tau)]} \quad (6)$$

Divide the boundary Γ into M_e boundary elements and time t into N equal time intervals. Equation (5) becomes

$$aT(\vec{\xi},t) = \sum_{i=1}^{M_e}\int_{\Gamma_i}\left[\sum_{j=1}^{N}\int_{(j-1)\Delta t}^{j\Delta t} {}_iq(\vec{r},\tau)\, G(\vec{r}-\vec{\xi};N\Delta t-\tau)\mathrm{d}\tau\right]\mathrm{d}\vec{r} - \sum_{i=1}^{M_e}\int_{\Gamma_i}\left[\sum_{j=1}^{N}\int_{(j-1)\Delta t}^{j\Delta t} {}_iT(\vec{r},\tau)\, \vec{n}\vec{\nabla}G(\vec{r}-\vec{\xi};N\Delta t-\tau)\mathrm{d}\tau\right]\mathrm{d}\vec{r} \quad (7)$$

where front subscript denotes element index. Now, let's approximate ${}_iq$ and ${}_iT$ by piecewise linear functions in time.

$${}_iq(\vec{r},\tau) = \frac{1}{\Delta t}\left[{}_iq^{(j)}(\vec{r}) - {}_iq^{(j-1)}(\vec{r})\right](\tau - N\Delta t) + {}_iq^{(j)}(\vec{r})(N-j+1) - {}_iq^{(j-1)}(\vec{r})(N-j) \quad (8)$$

$${}_iT(\vec{r},\tau) = \frac{1}{\Delta t}\left[{}_iT^{(j)}(\vec{r}) - {}_iT^{(j-1)}(\vec{r})\right](\tau - N\Delta t) + {}_iT^{(j)}(\vec{r})(N-j+1) - {}_iT^{(j-1)}(\vec{r})(N-j) \quad (9)$$

where superscript denotes time index. Next, approximate ${}_iq^{(j)}$ and ${}_iT^{(j)}$ over element i, making use of interpolating function Φ_k, as follows.

$${}_iq^{(j)}(\vec{r}) = \sum_{k=1}^{L} {}_{i,k}q^{(j)}\Phi_k(\vec{r}) \quad (10)$$

$${}_iT^{(j)}(\vec{r}) = \sum_{k=1}^{L} {}_{i,k}T^{(j)}\Phi_k(\vec{r}) \quad (11)$$

where k is local node index, and L is the number of nodes in an element. Substituting equations (8)-(11) into equation (7) yields

$$\begin{aligned} aT(\vec{\xi},t) = {} & \sum_{i=1}^{M_e}\sum_{k=1}^{L}\left\{\int_{\Gamma_i}\left[\sum_{j=1}^{N}\int_{(j-1)\Delta t}^{j\Delta t}\left(\frac{(\tau-N\Delta t)}{\Delta t}+(N-j+1)\right)G\mathrm{d}\tau\right]\Phi_k(\vec{r})\mathrm{d}\vec{r}\right\}\left({}_{i,k}q^{(j)}\right) \\ & - \sum_{i=1}^{M_e}\sum_{k=1}^{L}\left\{\int_{\Gamma_i}\left[\sum_{j=1}^{N}\int_{(j-1)\Delta t}^{j\Delta t}\left(\frac{(\tau-N\Delta t)}{\Delta t}+(N-j)\right)G\mathrm{d}\tau\right]\Phi_k(\vec{r})\mathrm{d}\vec{r}\right\}\left({}_{i,k}q^{(j-1)}\right) \\ & - \sum_{i=1}^{M_e}\sum_{k=1}^{L}\left\{\int_{\Gamma_i}\left[\sum_{j=1}^{N}\int_{(j-1)\Delta t}^{j\Delta t}\left(\frac{(\tau-N\Delta t)}{\Delta t}+(N-j+1)\right)\vec{n}\vec{\nabla}G\mathrm{d}\tau\right]\Phi_k(\vec{r})\mathrm{d}\vec{r}\right\}\left({}_{i,k}T^{(j)}\right) \\ & + \sum_{i=1}^{M_e}\sum_{k=1}^{L}\left\{\int_{\Gamma_i}\left[\sum_{j=1}^{N}\int_{(j-1)\Delta t}^{j\Delta t}\left(\frac{(\tau-N\Delta t)}{\Delta t}+(N-j)\right)\vec{n}\vec{\nabla}G\mathrm{d}\tau\right]\Phi_k(\vec{r})\mathrm{d}\vec{r}\right\}\left({}_{i,k}T^{(j-1)}\right) \end{aligned} \quad (12)$$

If equation (12) is evaluated at a point $\vec{\xi}_k$ on the boundary or inside the object, the resulting equation after the assembly process can be written as

$$a_k T_k^{(N)} = \sum_{j=1}^{N}\sum_{i=1}^{M_n} \phi\left(\vec{\xi}_k, \vec{r}_i, (N-j)\Delta t\right) T_i^{(j)} + \sum_{j=1}^{N}\sum_{i=1}^{M_n+M_c} \psi\left(\vec{\xi}_k, \vec{r}_i, (N-j)\Delta t\right) q_i^{(j)} \quad (13)$$

where back subscript denotes global node index, M_n is the number of boundary nodes, and M_c is the number of additional heat flux components at corner or edge nodes. Note that coefficient a_k becomes unity if $\vec{\xi}_k$ is inside the object. For two-dimensional problems, each corner node can have two heat flux components; therefore, M_c is equal to the number of corners. Functions ϕ and ψ are obtained from the evaluation of integrals shown in equation (12). The evaluation of time integrals can be done exactly as shown in the Appendix, while the evaluation of boundary integrals should be performed using the Gaussian quadrature.

Equation (13) is now written for M_n boundary node points, yielding M_n equations that relate boundary temperatures to boundary heat flux components. The resulting equations may be expressed as the following two matrix equations.

$$A\vec{T}^{(N)} = \sum_{j=1}^{N} P_1^{(N-j)}\vec{T}^{(j)} + \sum_{j=1}^{N} R_1^{(N-j)}\vec{q}^{(j)} + \sum_{j=1}^{N} S_1^{(N-j)}\vec{g}^{(j)} \quad (14)$$

$$\vec{f}^{(N)} = \sum_{j=1}^{N} P_2^{(N-j)}\vec{T}^{(j)} + \sum_{j=1}^{N} R_2^{(N-j)}\vec{q}^{(j)} + \sum_{j=1}^{N} S_2^{(N-j)}\vec{g}^{(j)} \quad (15)$$

where A is diagonal matrix of coefficients a; $\vec{T}$ is the vector of temperatures on the boundary; $\vec{f}$ is the vector of temperatures inside the object; $\vec{q}$ is the vector of boundary heat flux components that are to be determined; $\vec{g}$ is the vector of specified boundary heat flux components; P_1 and P_2 are coefficient matrices consisting of ψ functions; and R_1, R_2, S_1, and S_2 are coefficient matrices consisting of ϕ functions.Let $\vec{T}_0$ and $\vec{f}_0$ be, respectively, the boundary and interior temperature responses when $\vec{q} = 0$.

$$A\vec{T}_0^{(N)} = \sum_{j=1}^{N} P_1^{(N-j)}\vec{T}_0^{(j)} + \sum_{j=1}^{N} S_1^{(N-j)}\vec{g}^{(j)} \quad (16)$$

$$\vec{f}_0^{(N)} = \sum_{j=1}^{N} P_2^{(N-j)}\vec{T}_0^{(j)} + \sum_{j=1}^{N} S_2^{(N-j)}\vec{g}^{(j)} \quad (17)$$

If $\vec{g}$ is known as a function of time, $\vec{T}_0$ and $\vec{f}_0$ can be determined by the time-stepping procedure. Subtracting equations (16) from (14) and (17) from (15) results in

$$A\left[\vec{T}^{(N)} - \vec{T}_0^{(N)}\right] = \sum_{j=1}^{N} P_1^{(N-j)}\left[\vec{T}^{(j)} - \vec{T}_0^{(j)}\right] + \sum_{j=1}^{N} R_1^{(N-j)}\vec{q}^{(j)} \quad (18)$$

$$\left[\vec{f}^{(N)} - \vec{f}_0^{(N)}\right] = \sum_{j=1}^{N} P_2^{(N-j)}\left[\vec{f}^{(j)} - \vec{f}_0^{(j)}\right] + \sum_{j=1}^{N} R_2^{(N-j)}\vec{q}^{(j)} \quad (19)$$

Applying the time-stepping procedure to equations (18) and (19) gives us the following relations between boundary and interior temperatures and the unknown boundary heat flux.

$$\vec{T}^{(k)} - \vec{T}_0^{(k)} = \sum_{j=1}^{k} X_1^{(j-k)}\vec{q}^{(k)} \quad (20)$$

$$\vec{f}^{(k)} - \vec{f}_0^{(k)} = \sum_{j=1}^{k} X_2^{(j-k)}\vec{q}^{(k)} \quad (21)$$

Of the M_n equations for boundary temperatures in the matrix equation (20), only M_1 equations, corresponding to M_1 boundary sensor locations, are to be used for the determination of boundary heat flux. These equations are combined with M_2 equations represented by the matrix equation (21). The result can be written as

$$\vec{Y}^{(k)} - \vec{Y}_0^{(k)} = \sum_{j=1}^{k} X^{(k-j)}\vec{q}^{(j)} \quad (22)$$

where $\vec{Y}^{(k)}$ is the vector of temperature measurements on the boundary and inside the object at time $k\Delta t$, and $\vec{Y}_0^{(k)}$ is the vector temperatures at these sensor locations when $\vec{q} = 0$ from time 0 to $k\Delta t$.

It is expedient to express estimated heat flux vector at time level k in terms of temperature measurements from time level 1 to k as follows.

$$\vec{q}^{(k)} = \sum_{j=1}^{k} D^{(k-j)}\left[\vec{Y}^{(j)} - \vec{Y}_0^{(j)}\right] \quad (23)$$

where D is the coefficient matrix relating estimated heat flux to measured temperatures.

From simple algebra, it can be shown that D is related to X in the following manner.

$$X^{(0)}D^{(0)} = \mathrm{I} \quad (24)$$

where I is the identity matrix.

$$X^{(0)}D^{(k)} = -\sum_{j=0}^{k-1} X^{(k-j)}D^{(j)} \quad (25)$$

for $k > 0$.

The dimensions of D and X depend on the numbers of unknown heat flux components and measured temperatures. If the suggestion by Beck et al. [1] that the number of temperature sensors should be equal to or greater than the number of unknown heat flux components is followed, matrices D and X may be rectangular matrices, and solutions to Eqs. (24) and (25) have to be obtained using the linear least squares method. For the purpose of getting such solutions, the subroutine dgelss.f in the numerical package LAPACK (which is available at http://www.netlib.org/lapack) may be used.

Once all coefficient matrices are known, the unknown heat flux can be estimated from Eq. (23). Normally, temperature measurements contain statistical errors, which will result in the statistical errors in estimated heat flux. If it is assumed that errors in temperature measurements have uniform variance σ^2, are normally distributed, and are uncorrelated, the variance in estimated heat flux is given by

$$\mathrm{Var}(q_i^{(k)}) = \sigma^2 \sum_{l=1}^{k} \sum_{j=1}^{N} \left(D_{ij}^{(k-l)}\right)^2 \quad (26)$$

The characteristic of the solution to the IHCP is such that the variance of the estimate becomes larger as the estimated heat flux approximates the true heat flux better. Conversely, it may be necessary to accept a larger deviation between the true heat flux and the estimated heat flux in order to reduce the variance of the solution.

4. Results and Discussion

The sample problem is illustrated in Fig. 1. A square object of length 1.0, which is insulated on three sides, is subjected to unknown heat flux on the remaining side AB. The unknown heat flux will be determined using the algorithm described earlier with temperature sensors located inside the object or on its boundary.

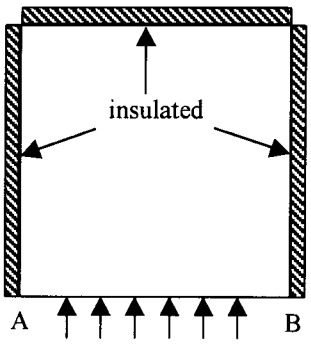

Figure 1: Sample problem

For computational purpose, the boundary is divided uniformly into 48 linear elements. It was found from a numerical test that the L_2 norm of the difference between computed solution and exact solution is only about 0.4% of the exact solution. Furthermore, the L_2 norm of this difference monotonically decreased as more elements were used. Hence, the numerical algorithm appears to have satisfactory accuracy.

Since only surface AB is non-insulated, only the heat flux components on 13 nodes along AB are to be estimated. This problem is simplified by the fact that $\vec{g} = 0$. Hence, $\vec{Y}_0$ vanishes. The time step used is 0.1, and the calculation is performed from time 0 to 1.0.

For a corresponding direct problem (i.e. one in which boundary heat flux is known, and temperature distribution is to be determined) with the boundary heat flux illustrated in Fig. 2, the exact solution for temperature distribution is given by

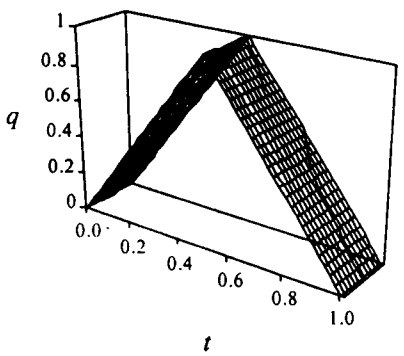

Figure 2: Actual boundary heat flux

$$T(x,t) = \begin{cases} 2U(x,t), & \text{for } t \le 0.5 \\ 2U(x,t) - 4U(x,t-0.5), & \text{for } t > 0.5 \end{cases}$$

where

$$U(x,t) = \frac{1}{\Delta t}\left[\frac{t^2}{2} + t\left(\frac{x^2}{2} - x + \frac{1}{3}\right) - 2\sum_{j=1}^{\infty}\frac{\cos(j\pi x)}{(j\pi)^4}\left(1 - e^{-j^2\pi^2 t}\right)\right] \quad (27)$$

The solution to this direct problem will be now used to supply input to the inverse problem. The calculated heat flux can then be compared with Fig. 2. This comparison, together with the variance of the estimate as given in Eq. (26), will be used to assess the quality of the solution

Three factors play a dominant role in affecting the solution of this inverse problem. They are (1) the number of heat flux components to be estimated, (2) the number of temperature sensors, and (3) the locations of the sensors. In order to see the influence of each factor, three cases will be considered.

4.1 Case 1: Influence of the number of heat flux components

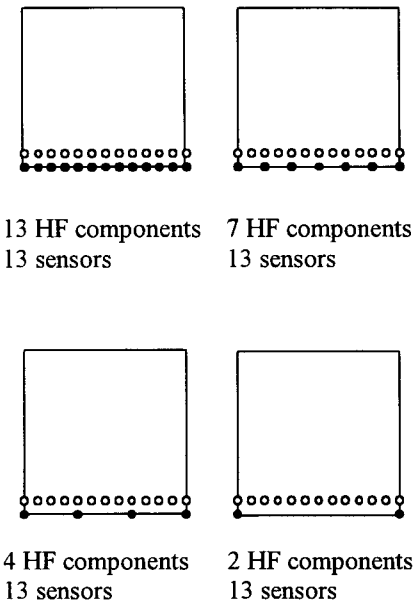

Figure 3: The numbers of HF components and sensors in Case 1 (• represents location of HF component and ▫ represents location of sensor)

Due to the mesh generation used, there are at most 13 heat flux components to be estimated. However, the solution to the problem may seek to estimate fewer than 13 heat flux components, and assume that the remaining components are determined by interpolation from estimated components. Fig. 3 shows 4 different sub-cases. The numbers of HF components / sensors in these cases are 13 / 13, 7 / 13, 4 / 13, and 2 / 13.

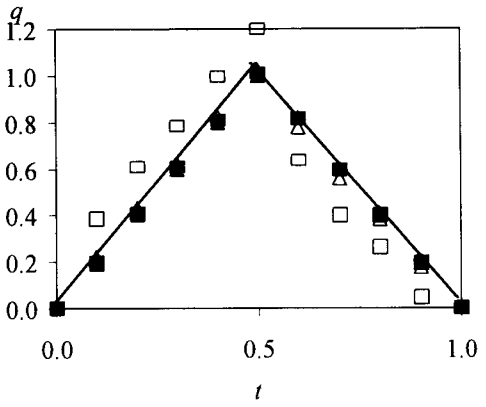

Figure 4: Solutions for the heat flux component at A in Case 1. Solid line is the actual heat flux. Squares, triangles, solid squares, and solid triangle represent solutions in sub-cases of 13, 7, 4, and 2 heat flux components, respectively.

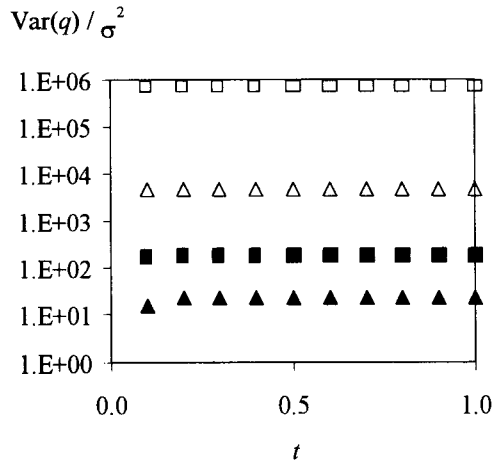

Figure 5: Variance of the estimated heat flux component at A in Case 1. Squares, triangles, solid squares, and solid triangle represent solutions in sub-cases of 13, 7, 4, and 2 heat flux

components, respectively. Note that σ^2 is the variance in temperature measurements.

In order to compare solutions from the four different sub-cases, it is necessary to consider a common heat flux component. Inspection of Fig. 3 reveals that the common heat flux components are those at left end (A) or right end (B). Comparison of the solutions for the heat flux component at either location should be sufficient. Figure 4 shows the comparison of the solutions for the heat flux component at A. It can be seen that when there are too many heat flux components to be estimated, the solution will deviate noticeably from the actual heat flux. Although it is difficult to tell from the figure, the results of computations indicat that the fewer the heat flux components, the more closely the solution resembles the actual heat flux.

In addition to yielding a less accurate solution, Fig. 5 shows that a higher number of estimated heat flux components also results in a higher variance of the solution. In other words, the solution will be more sensitive to temperature measurement errors if the number of estimated heat flux components increases.

4.2 Case 2: Influence of the number of temperature sensors

The number of sensors must be greater than or equal to the number of heat flux components. Here there are two heat flux components to be estimated, and four sub-cases of different numbers of sensors. As shown in Fig. 6, the numbers of heat flux components / sensors in these cases are 2 / 13, 2 / 7, 2 / 4, and 2 / 2.

Figure 7 shows that the solutions from all sub-cases are similar. The computational results must be closely inspected to see the small differences in solutions, with sub-cases having a higher number of sensors yielding slightly more accurate solutions. The influence of the number of sensors on variance of solution is more noticeable. Figure 8 shows that the higher number of sensors leads to a solution that is less sensitive to measurement errors.

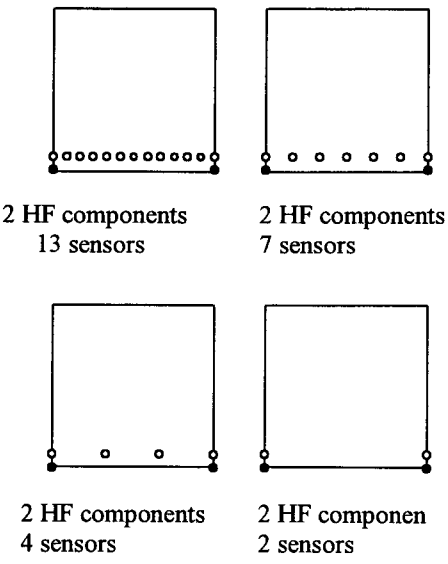

Figure 6: The numbers of HF components and sensors in Case 2 (• represents location of HF component and ○ represents location of sensor)

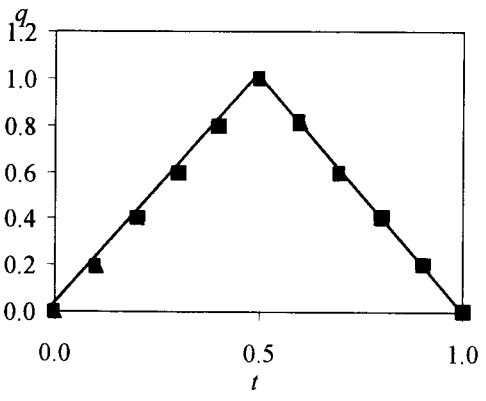

Figure 7: Solutions for the heat flux component at A in Case 2. Solid line is the actual heat flux. All sub-cases yield similar solutions, represented by solid squares.

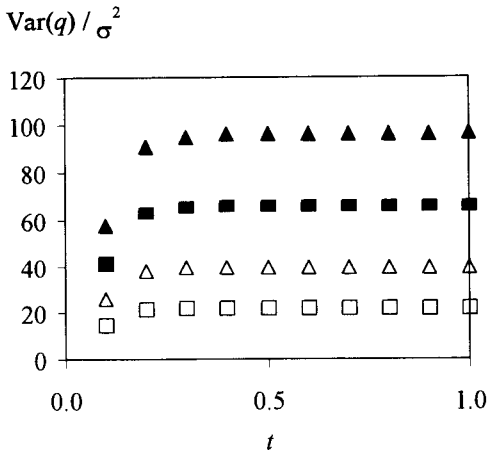

Figure 8: Variance of the estimated heat flux component at A in Case 2. Squares, triangles, solid squares, and solid triangle represent solutions in sub-cases of 13, 7, 4, and 2 sensors, respectively. Note that σ^2 is the variance in temperature measurements.

4.3 Case 3: Influence of the locations of temperature sensors

If the numbers of sensors and heat flux components are fixed, the locations of sensors have a great influence on the estimated heat flux. There are 2 heat flux components and 13 sensors in Case 3. But each of the 4 sub-cases is associated with a different location of sensors, as shown in Fig. 9.

It can be seen from Figs. 10 and 11 that the effects of the locations of sensors are such that the solution becomes both less accurate and more sensitive to errors in temperature measurements as the sensors are located farther away from the boundary of unknown heat flux. In fact, when x = 1/2 or 3/4, the solution is unacceptable because it is very different from the actual solution, and the variance is too large.

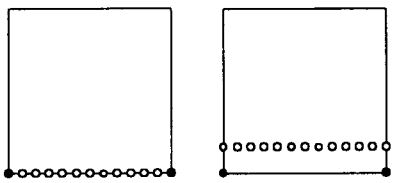

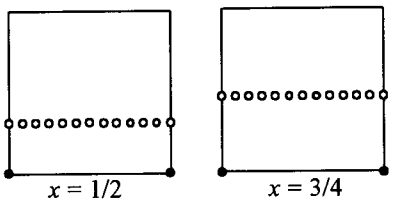

Figure 9: The locations of sensors in Case 3 (x is the distance from the bottom boundary to sensors, • represents location of HF component and ○ represents location of sensor).

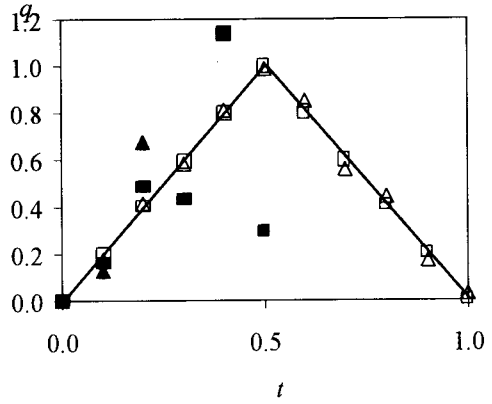

Figure 10: Solutions for the heat flux component at A in Case 3. Solid line is the actual heat flux. Squares, triangles, solid squares, and solid triangle represent solutions in sub-cases of x = 0, 1/4, 1/2, and 3/4, respectively. Results for x = 1/2 and 3/4 no longer resemble the actual heat flux.

5. Conclusions

The boundary element method is used to solve the inverse heat conduction problem, which is the determination of boundary heat flux from temperature measurements, in two dimensions. Like the finite element method, this method can deal with arbitrary geometry. However, unlike the finite element method, it is more computationally efficient since it does not require domain mesh generation.

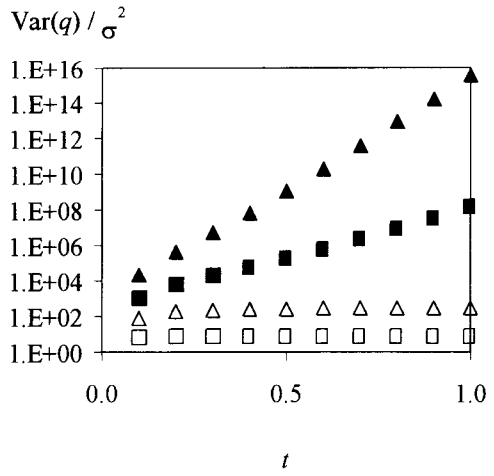

Figure 11: Variance of the estimated heat flux component at A in Case 3. Squares, triangles, solid squares, and solid triangle represent solutions in sub-cases of x = 0, 1/4, 1/2, and 3/4, respectively. Note that σ^2 is the variance in temperature measurements.

The quality of the solution is a function of how close the estimated heat flux to the actual heat flux and how sensitive the solution is to errors in temperature measurements. It is influenced by three important factors _ the number of heat flux components to be estimated, the number of temperature sensors, and the locations of the sensors. Increasing the number of heat flux components, decreasing the number of sensors, or increasing the distance between sensors and boundary of unknown heat flux leads to a poorer quality.

The results from this paper should provide some guidance to future experimental work. In order for the experiment in determining heat flux from temperature measurements to be successful, it should be designed in such a way that the number of unknown heat flux components is minimized, the number of sensors is maximized, and the sensors are located as close to the boundary of unknown heat flux as practical.

6. Acknowledgement

The author would like to acknowledge financial support from the Thailand Research Fund.

7. References

[1] Beck, J. V., Blackwell, B., and St. Clair, C. R., Jr., Inverse Heat Conduction: Ill-posed Problems, Wiley-Interscience Pub., New York, 1985.

[2] Lesnic, D., Elliott, L., and Ingham, D. B., Application of the Boundary Element Method to Inverse Heat Conduction Problems, International Journal of Heat and Mass Transfer, Vol. 39, No. 7, pp. 1503-1517, 1996.

[3] Sassi, M. and Raynaud, M., New Space-marching Method for Solving Inverse Boundary Problems, Numerical Heat Transfer, Part B, Vol. 34, No. 1, pp. 21-38, 1998.

[4] Elden, L., Solving an Inverse Heat Conduction Problem by a Method of Lines, Journal of Heat Transfer, Vol. 119, No. 3, pp. 406-412, 1997.

[5] Reinhardt, H. J., A Numerical Method for the Solution of Two-dimensional Inverse Heat Conduction Problems, International Journal for Numerical Methods in Engineering, Vol. 32, No. 2, pp. 363-383, 1991.

[6] Osman, A. M., Dowding, K. J., and Beck, J. V., Numerical Solution of the General Two-dimensional Inverse Heat Conduction Problem (IHCP), Journal of Heat Transfer, Vol. 119, No. 1, pp. 38-45, 1997.

[7] Al-Khalidy, N., A General Space Marching Algorithm for the Solution of Two-dimensional Boundary Inverse Heat Conduction Problems, Numerical Heat Transfer, Part B, Vol. 34, No. 3, pp. 339-360, 1998.

[8] Tseng, A. A., Chen, T. C., and Zhao, F. Z., Direct Sensitivity Coefficient Method for Solving Two-dimensional Inverse Heat Conduction Problems by Finite-element Scheme, Numerical Heat Transfer, Part B, Vol. 27, No. 3, pp. 291-307, 1995.

[9] Al-Najem, N. M., Osman, A. M., El-Refaee, M. M., and Khanafer, K. M., Two Dimensional Steady-state Inverse Heat Conduction Problems, International Communications in Heat and Mass Transfer, Vol. 25, No. 4, pp. 541-550, 1998.

[10] Banerjee, P. K. and Butterfield, R., Boundary Element Methods in Engineering Science, McGraw-Hill, London, 1981.